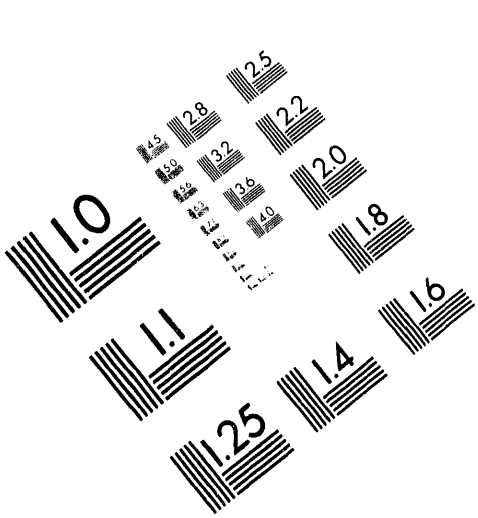

Association for Information and Image Management
1100 Wayne Avenue, Suite 1100
Silver Spring, Maryland 20910
301/587-8202

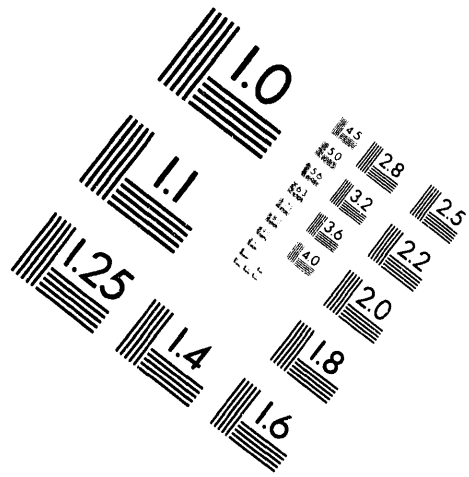

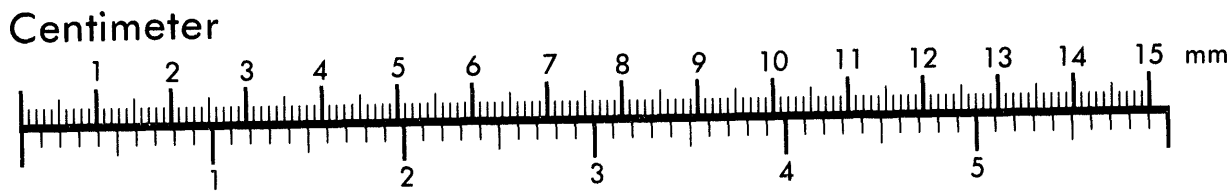

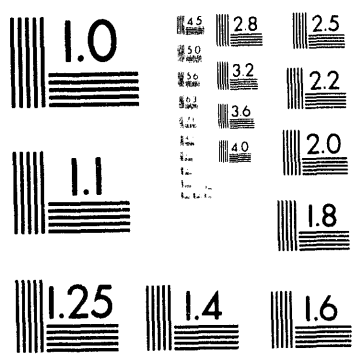

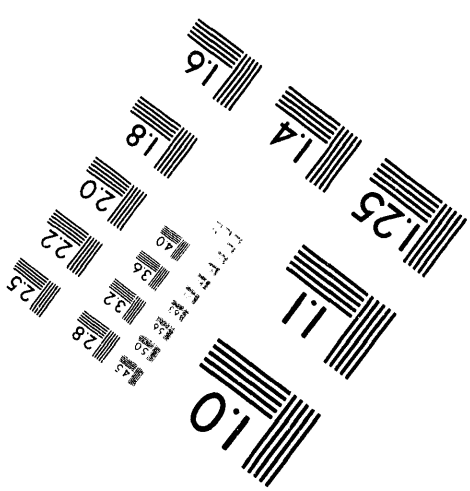

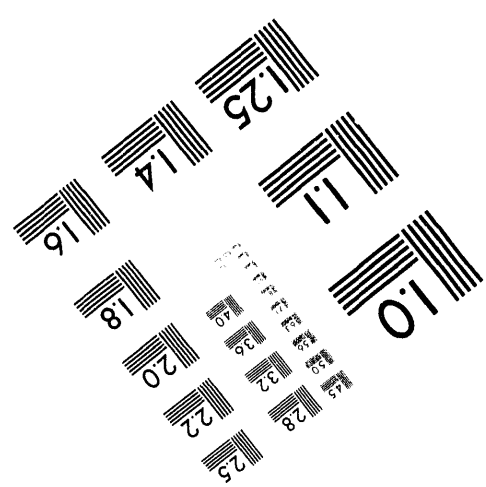

MANUFACTURED TO AIIM STANDARDS
BY APPLIED IMAGE, INC.

1 of 1

SAND94-1019C

Residual Stress and Raman Spectra of Laser Deposited Highly-Tetrahedral-Coordinated-Amorphous-Carbon Films

CONF-940411--18

T. A. Friedmann, M. P. Siegal, D. R. Tallant, R. L. Simpson, and F. Dominguez
Sandia National Laboratories, Albuquerque, NM 87185

ABSTRACT

We are studying carbon thin films by using a pulsed excimer laser to ablate pyrolytic graphite targets to form highly tetrahedral coordinated amorphous carbon (αt-C) films. These films have been grown on room temperature p-type Si (100) substrates without the intentional incorporation of hydrogen. In order to understand and optimize the growth of αt-C films, parametric studies of the growth parameters have been performed. We have also introduced various background gases (H_2, N_2 and Ar) and varied the background gas pressure during deposition. The residual compressive stress levels in the films have been measured and correlated to changes in the Raman spectra of the αt-C band near 1565 cm^{-1}. The residual compressive stress falls with gas pressure, indicating a decreasing atomic sp^3-bonded carbon fraction. We find that reactive gases such as hydrogen and nitrogen significantly alter the Raman spectra at higher pressures. These effects are due to a combination of chemical incorporation of nitrogen and hydrogen into the film as well as collisional cooling of the ablation plume. In contrast, films grown in non-reactive Ar background gases show much less dramatic changes in the Raman spectra at similar pressures.

INTRODUCTION

In recent years, much attention has been focused on the growth of amorphous-diamond-like-carbon films containing hydrogen (aC:H). Such films are usually grown by a plasma CVD method using methane gas as the carbon source. This process produces films that contain large amounts of hydrogen (20 - 70 atomic percentage) with C-H bonds accounting for the high tetrahedral coordination of the carbon atoms.

More recently, several methods have been developed to deposit highly-tetrahedral-coordinated-amorphous-carbon (αt-C) films without intentionally adding hydrogen. The tetrahedral coordination in these films is mainly due to C-C bonding. The methods used to produce these films include the filtered cathodic arc[1, 2], ion beam deposition[3, 4], and pulsed laser deposition (PLD)[5-10]. We are studying αt-C films produced by PLD. The resultant films grown by these processes show a high hardness, thermal stability over a wider temperature range than aC:H films[11], and better electronic properties[12, 13]. The successful methods for growing αt-C films require the presence of an activated carbon source (carbon atoms, ions, or clusters of energies ranging from 20 to 1000 eV) to produce high quality films (> 70% sp^3-bonded C). This suggests that a common mechanism is responsible for the production of the αt-C phase.

McKenzie et al[14, 15] proposed that internal compressive stress is generated in the growing film by the sub-surface implantation of the impinging carbon species. This compressive stress raises the growing film surface to the point in the diamond pressure-temperature phase diagram were the formation of sp^3 bonds is favored. This model predicts that the residual stress should correlate with the sp^3-content in αt-C films. Davis[16] has shown how the dynamic creation and annihilation of vacancies and interstitials during ion bombardment can lead to the buildup of stress during film deposition. The actual stress level is sensitive to the ion energy. Therefore, any process that affects the kinetic energy of the depositing carbon species should also affect the residual compressive stress in the film. One means of modifying the energy of the carbon species is through the addition of a background gas during deposition.

DISTRIBUTION OF THIS DOCUMENT IS UNLIMITED

MASTER

In this paper, we report on our observations of the residual stress in αt-C films grown in three different ambient background gases (H_2, N_2 and Ar) and correlate these stresses with Raman spectra of the resultant films.

EXPERIMENTAL

The PLD vacuum chamber (Fig. 1) is capable of attaining a base pressure of 1 x 10^{-8} Torr. The pyrolytic graphite targets (Union Carbide) were ablated with a KrF (248 nm) laser capable of generating 450 mJ pulses of 17 ns duration. The deposition time was held constant at 20 minutes at a laser repetition rate of 20 Hz. The laser light was focused into the vacuum chamber using a spherical lens with a 35 cm focal length. The laser beam illuminates the rotating target at a 45° angle from the target normal. The beam forms a rectangular spot on the target with an area of 0.01 cm^2 corresponding to an energy density of 45 J/cm^2. The ablated plume is ejected perpendicular to the target and deposits on a rotating substrate 10 cm away and parallel to the target. Before deposition, the silicon (100) substrates (p-doped with B to 20 - 50 Ωcm) were cleaned to remove the surface oxide layer by a wet dip procedure in a HF/NH_4F solution[17]. The rotating Si substrates were not actively heated during deposition, although some residual heating (< 50 °C) occurred due to the condensation of energetic species from the plume. During deposition, background gases composed of H_2, N_2 and Ar could be fed into the chamber and their pressure controlled by a throttle valve and measured with a capacitance based pressure transducer capable of reading absolute pressure. In this manner background pressures could be regulated from the base pressure of the chamber up to 1 Torr of gas pressure.

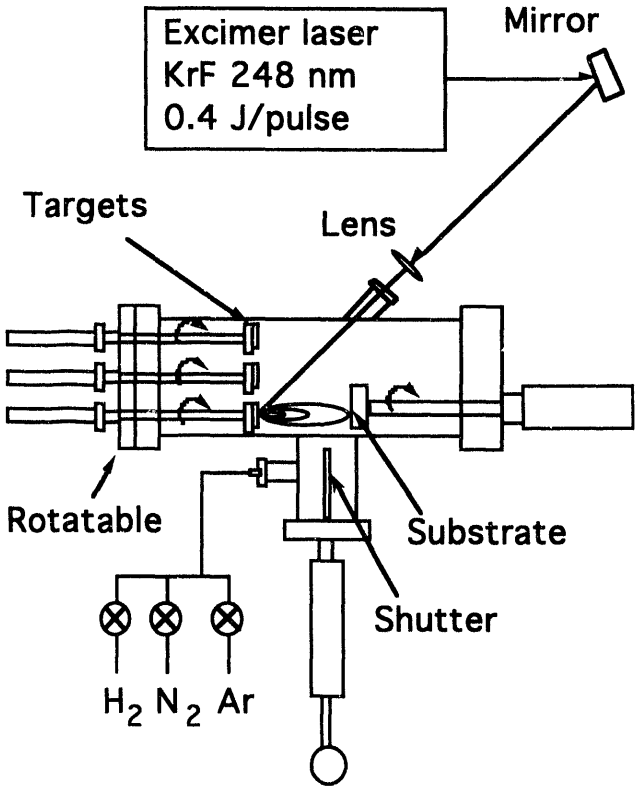

Fig. 1 A diagram of the chamber used to deposit the films.

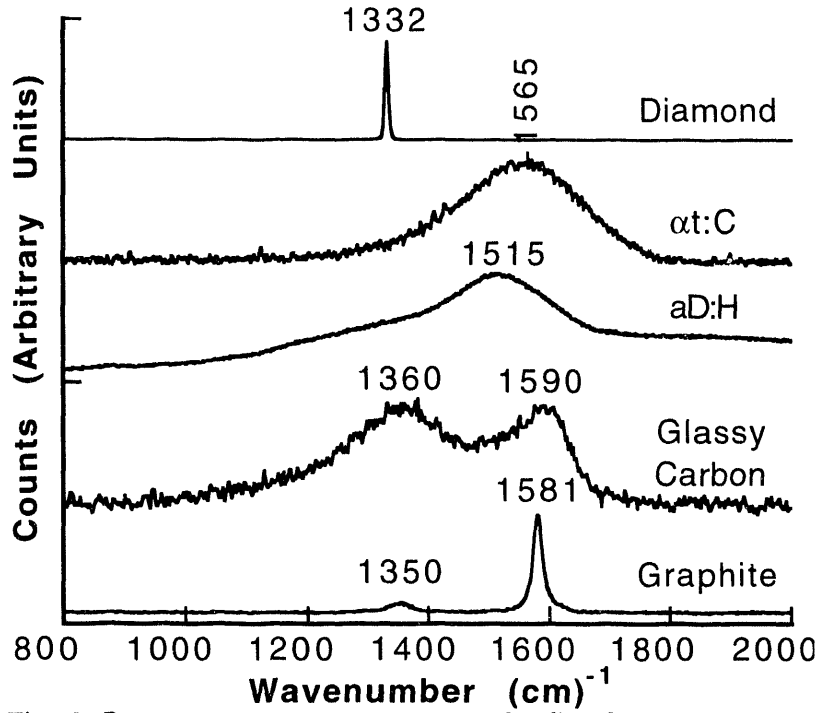

Fig. 2 Representative Raman spectra for five forms of carbon. Note the difference in peak position and shape between the αt-C and aC:H spectra.

Characterization of the samples was accomplished mainly through Raman spectroscopy, which serves to differentiate between various forms of carbon. The films were measured with 514 nm light at 50 mW of power. Fig. 2 depicts five Raman spectra of different forms of carbon

ranging from graphite to diamond. For graphite there are two active modes at 1350 cm^{-1} and 1581 cm^{-1}, due to the out-of-plane and in-plane vibration modes characteristic of sp^2-bonded carbon. Glassy carbon is a disordered graphitic phase with broad Raman peaks near 1360 cm^{-1} and 1590 cm^{-1}. Diamond has one active Raman mode at 1332 cm^{-1} characteristic of sp^3-bonded carbon. Conventional aC:H has a broad asymmetric Raman peak near 1515 cm^{-1} with a long tail that extends down to ~1000 cm^{-1}. αt-C also has a single broad Raman mode, but this mode is shifted up to higher wavenumber (1565 cm^{-1}) and is more symmetric than that of aC:H. This peak arises from sp^2-bonded carbon atoms. The presence of sp^3-bonded carbon is not obvious in these spectra due to the resonance enhancement of the sp^2-bonded atoms at the laser wavelength used. Thus, the signal from sp^2-bonded carbon atoms overwhelms any signal due to sp^3-bonded carbon atoms making it difficult to determine the actual sp^3 content of the film from Raman measurements.

The wafer curvatures before and after deposition as well as the sample thicknesses were measured using a stylus profilometer. The residual stresses in the films, σ_f, could then be calculated using[18, 19]:

$$\sigma_f = \frac{E_s t_s^2}{6(1-\upsilon)t_f R} \tag{1}$$

where E_s is Young's modulus for the substrate, υ is Poisson's ratio for the substrate[20], t_s is the substrate thickness, t_f is the film thickness, and R is the radius of curvature. For the films grown in this study the residual stress was always compressive.

A parametric study was undertaken in order to optimize the deposition process and produce films with varying levels of stress. Samples were deposited using varying background gases at varying pressure. The present paper focuses on the changes in residual stress and in the Raman spectra as a function of background gas pressure.

DISCUSSION

Fig. 3 depicts the residual stress versus pressure for samples grown in an Ar ambient gas. The film grown in vacuum shows a residual stress level near 8 GPa. This high level of stress limits the maximum film thickness (~3000 Å) due to stress induced spalling of the film. The residual stress decreases linearly with increasing Ar pressure. At these lower stress levels the films can be grown thicker (>3000 Å) before spalling from the substrate. The reduction in residual stress with pressure is probably due to collisional cooling of the ablated plume by the ambient background gas. The average energy distribution of carbon species in the plume would be reduced and broadened. This would reduce the stress in the growing film by reducing the number of vacancies and interstitials produced upon impact, and consequently reducing the sp^3 content of the films. However, it must be noted that the deposition rate also decreases with increasing gas pressure (from ~1.0 Å/s to ~0.2 Å/s over the pressure range studied) so that films grown at higher pressures are thinner and experience a lower fluence than those grown in vacuum. The lower fluence at higher pressures may also contribute to the stress reduction, since the dynamics of the stress formation process

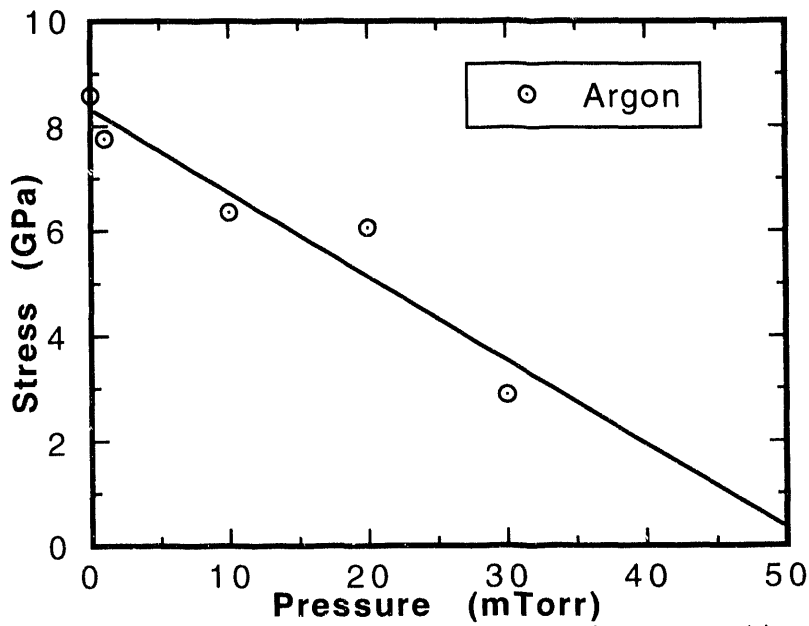

Fig. 3 Stress vs. Pressure for samples grown in an Ar ambient gas.

(creation and annihilation of vacancies and interstitials) will also be changed.

Fig. 4 depicts a plot of the residual stress versus pressure for samples deposited in hydrogen and nitrogen ambients. For hydrogen, a linear relationship between the stress and pressure is observed, very similar to the films grown in an Ar ambient gas. For nitrogen, there appears to be a break in the stress versus pressure curve near 20 mTorr of gas pressure; and the residual stress level falls faster than for H_2 or Ar. If the stress level correlates to the percentage of sp^3-bonded carbon atoms, then it appears that nitrogen is more effective in reducing the sp^3 content of the films. However, as will be shown below, both hydrogen and nitrogen are chemically incorporated into the films at these pressures. In the case of hydrogen incorporation, it is likely that C-H bonds maintain the high fraction of tetrahedrally coordinated carbon atoms (similar to aC:H). For the case of nitrogen incorporation, sp^2-bonded configurations are more likely, leading to a faster reduction in residual stress with pressure.

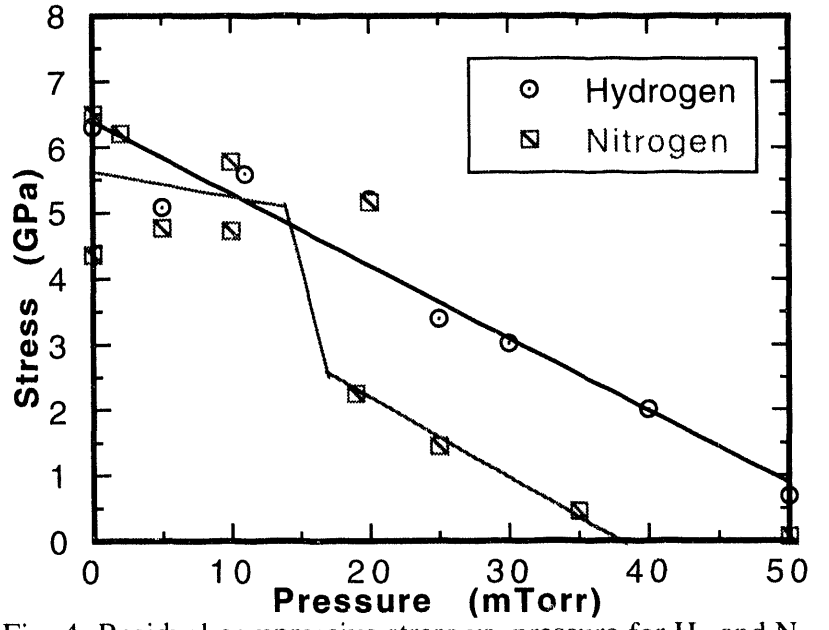

Fig. 4 Residual compressive stress vs. pressure for H_2 and N_2 background gases. Note the break in slope for the nitrogen data near 20 mTorr. The lines are drawn as guides to the eye.

To examine the nature of the bonding, Raman spectra were obtained from these films and are depicted in Fig. 5. Fig. 5a shows three representative Raman spectra from samples grown in an Ar ambient. The relatively sharp Raman band at ~950 cm^{-1} is due to the silicon substrate. As the Ar gas pressure increases, the silicon Raman band decreases in intensity indicating that the samples become less transparent. (Since the samples decrease in thickness at higher gas pressures, this effect is even greater than depicted in Fig. 5a.) This is consistent with the lower stress level observed at high gas pressure and is possibly due to increased absorption from graphitic elements in the film.

As the gas pressure increases, the αt-C Raman peak shifts from a relatively symmetric band near 1565 cm^{-1} to a broadened asymmetric band peaked near 1520 cm^{-1}. This change in peak shape and position reflects some change in bonding configuration and/or distribution for the sp^2-bonded carbon in the film. We speculate that collisional cooling may broaden the energy distribution of the ablated carbon species leading to a wider distribution of sp^2-bonded ring structures in the film.

Fig. 5b depicts representative Raman spectra taken from films deposited in a hydrogen background gas. The Raman spectra evolve smoothly with increasing H_2 pressure. This correlates well with the linear change in the stress with H_2 pressure. As is the case with the films deposited in Ar the intensity of the Si Raman band decreases (This is not apparent from Fig. 5b due to the increased scale of the graph.) with increasing gas pressure indicating that the films are more absorptive. The αt-C peak shifts down in wavenumber (from 1565 cm^{-1} to 1520 cm^{-1}) and also becomes dramatically more intense indicating that the Raman scattering efficiency is increasing. (The sample deposited in vacuum is plotted with the same intensity in Figs. 5a, 5b, and 5c) In addition, there is a distinct shoulder that develops near 1300 cm^{-1}. This shoulder does not appear for the samples deposited in Ar, and could be a result of hydrogen incorporation into the film, for it resembles the Raman spectra of aC:H shown in Fig. 2.

Fig. 5c depicts representative Raman spectra taken from films deposited in a nitrogen background gas. The silicon Raman band also decreases with increasing gas pressure indicating that the samples are more absorptive. The Raman spectra show a sharp increase in intensity above

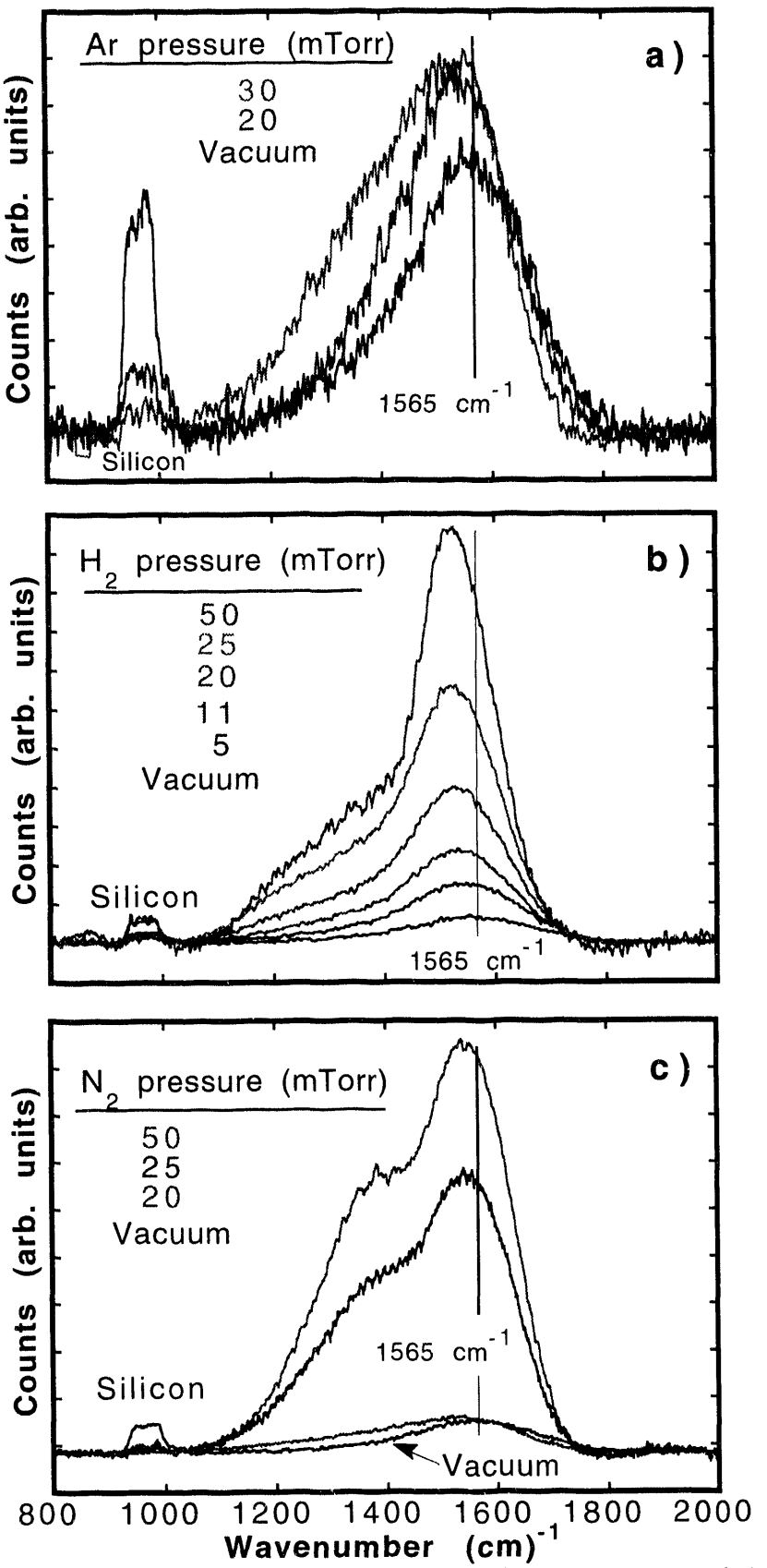

Fig. 5 Raman spectra for samples grown in a) Ar, b) H_2, and c) N_2 background ambients. Note that the spectrum for the sample grown in vacuum is plotted with the same intensity on each graph.

20 mTorr of gas pressure, which correlates with the break in residual stress with pressure noted above. In addition, the peak position of the αt-C Raman band shifts downward as the intensity of the band increases dramatically. A well developed shoulder also appears near 1380 cm^{-1}. This band is most likely due to nitrogen incorporation into the film and represents C-N bonding.

In general, we note that the Raman spectra show effects common to the presence of Ar, H_2, and N_2. These effects are increases in the Raman scattering efficiency, increases in absorption, and decreases in the αt-C peak position. To varying degree, these effects may be generically related to the increased gas pressure with a concomitant slowing of the laser-ablated carbon species and attenuation of their fluence. Changes of the αt-C line shape in N_2 and H_2 are most probably related to the chemical incorporation of these gases into the films, since these effects are dramatically different in the case of Ar.

Depositions were also undertaken in vacuum at varying laser energy densities[13]. At lower energy densities, the ejected carbon species should have a lower energy distribution, similar to the effect of adding a non reactive background gas. The resultant Raman spectra from these films are very similar to those grown in an Ar ambient gas.

CONCLUSIONS

We find that changes in the residual stress of films grown by pulsed laser deposition can be correlated with changes in the Raman spectra. In general, as the

pressure of the background gas increases the residual compressive stress in the films decreases. The Raman spectra show an increase in the Raman scattering efficiency, an increase in opacity, and a decrease in the peak position and symmetry of the αt-C Raman band. These effects may all be related to collisional cooling of the ablated carbon species by the background gas. In the case of Ar and H_2 ambients the change in stress with pressure was linear, and the resultant Raman spectra revealed a smooth evolution with pressure. In the case of a N_2 ambient, the stress changed abruptly with pressure near 20 mTorr; and the resultant Raman spectra showed a sharp increase in intensity and the development of a new band at 1380 cm^{-1} associated with the incorporation of nitrogen into the film.

ACKNOWLEDGMENT

This work was supported by the U.S. DOE under contract DE-AC04-94AL8500 through the Laboratory Directed Research and Development Program, Sandia National Laboratories.

REFERENCES

1. S. D. Berger, D. R. McKenzie, and P. J. Martin, Philos. Mag. Lett. **57**, 285 (1988).
2. R. Lossy, D. L. Pappas, R. A. Roy, and J. J. Cuomo, Appl. Phys. Lett. **61**, 171 (1992).
3. J. J. Cuomo, J. P. Doyle, J. Bruley, and J. C. Liu, J. Vac. Sci. Technol. A **9**, 2210 (1991).
4. C. Weissmantel, C. Shurer, F. Frohlich, P. Grau, and H. Lehmann, Thin Solid Films **61**, L5 (1979).
5. F. Xiong, Y. Y. Wang, V. Leppert, and R. P. H. Chang, J. Mater. Res. , (1993).
6. C. B. Collins, F. Davanloo, D. R. Jander, T. J. Lee, H. Park, and J. H. You, J. Appl. Phys. **69**, 7862 (1991).
7. F. Davanloo, E. M. Juengerman, D. R. Jander, T. J. Lee, and C. B. Collins, J. Appl. Phys. **67**, 2081 (1990).
8. J. Krishnaswamy, A. Rengan, J. Narayan, K. Vedam, and C. J. Mcharque, Appl. Phys. Lett. **54**, 2455 (1989).
9. C. L. Marquardt, R. T. Williams, and D. J. Nagel, in *Plasma Synthesis and Etching of Electronic Materials*, R. P. H. Chang, and B. Abeles, Eds. (Materials Research Society, Pittsburgh, 1985), vol. 38, pp. 325.
10. D. L. Pappas, K. L. Sanger, J. Bruley, W. Krakow, J. J. Cuomo, T. Gu, and R. W. Collins, J. Appl. Phys. **71**, 5675 (1992).
11. J. E. Parmeter, D. R. Tallant, and M. P. Siegal, in *Novel Forms of Carbon II*, C. L. Renschler, D. Cox, J. Pouch, and Y. Achiba, Eds. (Materials Research Society, Pittsburgh, 1994).
12. F. Xiong, Y. Y. .Wang, and R. P. H. Chang, Phys. Rev. B **48**, 8016 (1993).
13. M. J. Siegal, T. A. Friedmann, S. R. Kurtz, D. R. Tallant, R. L. Simpson, F. Dominguez, and K. F. McCarty, in *Novel Forms of Carbon II*, C. L. Renschler, D. Cox, J. Pouch, and Y. Achiba, Eds. (Materials Research Society, Pittsburgh, 1994).
14. D. R. McKenzie, D. Muller, and B. A. Pailthorpe, Phys. Rev. Lett. **67**, 773 (1991).
15. D. R. McKenzie, D. A. Muller, E. Kravtchinskaia, D. Segal, D. J. H. Cockayne, G. Amaratunga, and R. Silva, Thin Solid Films **206**, 198 (1991).
16. C. A. Davis, Thin Solid Films **226**, 30 (1993).
17. G. S. Higashi, Y. J. Chabal, G. W. Trucks, and K. Raghavachari, Appl. Phys. Lett. **56**, 656 (1990).
18. N. N. Davidenkov, Sov. Phys. Sol. State **2**, 2595 (1961).
19. R. W. Hoffman, Phys. Thin Films **3**, 211 (1966).
20. U. A. Brantley, J. Appl. Phys. **44**, 534 (1973).

DISCLAIMER

This report was prepared as an account of work sponsored by an agency of the United States Government. Neither the United States Government nor any agency thereof, nor any of their employees, makes any warranty, express or implied, or assumes any legal liability or responsibility for the accuracy, completeness, or usefulness of any information, apparatus, product, or process disclosed, or represents that its use would not infringe privately owned rights. Reference herein to any specific commercial product, process, or service by trade name, trademark, manufacturer, or otherwise does not necessarily constitute or imply its endorsement, recommendation, or favoring by the United States Government or any agency thereof. The views and opinions of authors expressed herein do not necessarily state or reflect those of the United States Government or any agency thereof.

DATE
FILMED
6/30/94

END